

# Natural Promoters of Calcium Oxalate Monohydrate Crystallization

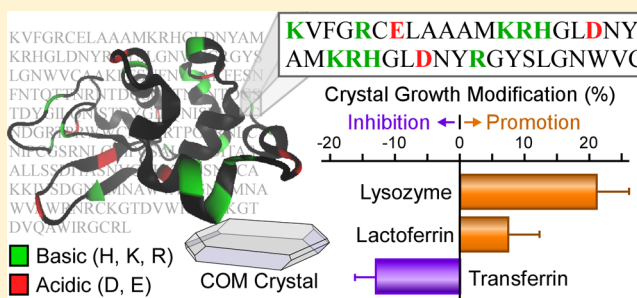
Sahar Farmanesh,<sup>†</sup> Jihae Chung,<sup>†</sup> Ricardo D. Sosa,<sup>†</sup> Jun Ha Kwak,<sup>‡</sup> Pankaj Karande,<sup>‡</sup> and Jeffrey D. Rimer<sup>\*†</sup>

<sup>†</sup>Department of Chemical and Biomolecular Engineering, University of Houston, Houston, Texas 77204, United States

<sup>‡</sup>Department of Chemical and Biological Engineering, Rensselaer Polytechnic Institute, Troy, New York 12180, United States

## Supporting Information

**ABSTRACT:** Crystallization is often facilitated by modifiers that interact with specific crystal surfaces and mediate the anisotropic rate of growth. Natural and synthetic modifiers tend to function as growth inhibitors that hinder solute attachment and impede the advancement of layers on crystal surfaces. There are fewer examples of modifiers that operate as growth promoters, whereby modifier–crystal interactions accelerate the kinetic rate of crystallization. Here, we examine two proteins, lysozyme and lactoferrin, which are observed in the organic matrix of three types of pathological stones: renal, prostatic, and pancreatic stones. This work focuses on the role of these proteins in the crystallization of calcium oxalate monohydrate (COM), the most prominent constituent of human kidney stones. Using a combination of experimental techniques, we show that these proteins, which are rich in L-arginine and L-lysine amino acids, promote COM growth. The synthesis and testing of peptides derived from contiguous segments of lysozyme's primary amino acid sequence revealed subdomains within the protein that operate either as an inhibitor or promoter of COM growth, with the latter exhibiting efficacies that nearly match that of the protein. We observed that cationic proteins promote COM growth over a wide range of modifier concentration, which differs from calcification promoters in the literature that exhibit dual roles as promoters and inhibitors at low and high concentration, respectively. This seems to suggest a unique mechanism of action for lysozyme and lactoferrin. Possible explanations for their effects on COM growth and crystal habit are proposed on the basis of classical colloidal theories and the physicochemical properties of peptide subdomains, including the number and spatial location of charged or hydrogen-bonding moieties.



## INTRODUCTION

The physical and chemical properties of crystalline materials can be tailored by incorporating ions, molecules, or macromolecules (often referred to as modifiers) in growth solutions. Modifiers bind to specific crystallographic faces and mediate the rate of anisotropic growth by either inhibiting or promoting the attachment of solute.<sup>1</sup> Nature provides many examples of such processes, which include the modification of minerals (e.g., calcium sulfate dihydrate<sup>2</sup>) and biogenic crystals (e.g., calcium carbonate in nacreous shells<sup>3–5</sup> and calcium phosphate in bone<sup>6</sup>). Modifiers in biomineralization are typically proteins, whereas the design of crystals *in vitro* often draws inspiration from nature through the use of biomimetic peptides, peptoids, polymers, and other organic molecules. The role of modifiers in natural and synthetic crystallization is generally that of an inhibitor that adsorbs at crystal interfaces and reduces the rate of growth.<sup>7–10</sup> There are fewer examples of growth promotion reported in the literature. The term *promotion* is often invoked to describe a wide range of phenomena, which include the modification of crystal size or number of nuclei,<sup>11–13</sup> the rate or degree of intercrystalline aggregation,<sup>14–16</sup> and the adsorption or epitaxial growth of crystals at interfaces.<sup>17</sup> Here, we

specifically refer to promotion as the ability of a modifier to accelerate the kinetic rate of crystal growth.

This study focuses on the modification of calcium oxalate monohydrate (COM), which is the most prevalent crystalline component of human renal stones.<sup>18,19</sup> It is well-established that many urinary proteins function as native inhibitors of COM crystallization. These inhibitors generally possess a high percentage of anionic functional groups, such as aspartic acid, glutamic acid, and phosphates.<sup>8,20–22</sup> One of the most widely studied inhibitors of COM is the urinary protein osteopontin (OPN)<sup>21,23–25</sup> as well as peptides derived from acid-rich segments of OPN.<sup>26,27</sup> Additional examples of natural COM growth inhibitors include citrate,<sup>21,28,29</sup> serum albumin,<sup>30</sup> and glycosaminoglycans (e.g., chondroitin sulfate).<sup>31</sup> In some instances, it is reported that modifiers exhibit dual roles as inhibitors and promoters, wherein their effect is based on modifier concentration, the pH or ionic strength of the growth solution, or modification to the amino acid sequence of a peptide/protein. Such effects have been reported for COM and other calcium minerals. For example, native protein G (an

Received: May 29, 2014

Published: August 13, 2014

immunoglobulin-binding protein)<sup>32</sup> is nominally a promoter of COM growth, but when aspartic acid and glutamic acid residues in protein G are substituted with asparagine and glutamine, respectively, the role of the protein switches to that of an inhibitor.<sup>32</sup> Studies of calcite (CaCO<sub>3</sub>) crystallization reveal that strontium is a growth promoter at low concentration but becomes a growth inhibitor at higher concentration (ca. 0.2 mM Sr<sup>2+</sup>).<sup>33</sup> Similar effects have been observed for peptide modifiers where the switch from calcite growth promoter to inhibitor occurs at much lower modifier concentration (ca. 0.1 μM peptide).<sup>34</sup>

Prior studies of COM growth modification have largely considered the effects of proteins with net negative charge. Interestingly, proteomic data from the analysis of organic constituents occluded within the matrix of COM stones<sup>35–37</sup> reveal proteins with net positive charge at physiological pH, 5–8,<sup>38</sup> yet the effect of cationic molecules on COM crystallization is less commonly investigated. Examples of urinary proteins with net positive charge include cathepsin G,<sup>38,39</sup> eosinophil cationic protein,<sup>38</sup> myeloperoxidase precursor,<sup>38,40</sup> histone-lysine *N*-methyltransferase, inward rectifier K channel, and protein Wnt-2.<sup>41</sup> These cationic proteins are rich in basic amino acid side chains, such as *L*-lysine, *L*-arginine, and *L*-histidine. Two cationic proteins of particular interest are lactoferrin<sup>38</sup> and lysozyme,<sup>38,39,42</sup> which are commonly found in renal and prostatic stones.<sup>43</sup> Lactoferrin has also been identified in the organic matrix of pancreatic stones,<sup>44</sup> while lysozyme concentration in urine is reportedly higher for individuals with renal diseases.<sup>45</sup> Despite their ubiquitous observation in pathological stones, the putative role of lactoferrin and lysozyme as crystal growth modifiers has yet to be established.

Herein, we explore the effects of lactoferrin and lysozyme on COM crystallization *in vitro* on the macroscopic and microscopic scales. We show that these proteins promote the rate of COM growth, with lysozyme having nearly twice the efficacy as that of lactoferrin. Kinetic studies of COM crystallization were performed in the presence of proteins, amino acids, and polyamino acids of varying size, net charge, and hydrophilicity. A systematic investigation of lysozyme was performed by synthesizing and testing the effects of 12 peptides derived from contiguous segments of the protein. Our findings reveal that smaller segments of lysozyme act as either promoters or inhibitors of COM crystal growth with similar efficacy as that of the larger protein. Bulk crystallization studies show that lysozyme and lactoferrin operate as growth promoters over a wide range of protein concentrations. This seems to suggest that these modifiers operate by a mechanism of action that differs from calcification promoters in the literature that exhibit dual promoter/inhibitor properties depending on their concentration.

## EXPERIMENTAL SECTION

Calcium oxalate monohydrate crystals were prepared according to a previously reported procedure.<sup>46</sup> Details of crystal preparation and peptide synthesis are provided in the Supporting Information.

COM crystals were analyzed by optical microscopy using a Leica DM2500-M microscope equipped with a video camera for recording. The crystal dimensions were measured in three directions (i.e., [001] length, [010] width, and [100] thickness). For each experiment, the dimension that is reported is an ensemble average of crystals measured from three separately prepared crystal batches. The zeta potential  $\zeta$  was measured with a NICOMP 380/ZLS instrument (Particle Sizing Systems, Santa Barbara, CA). All  $\zeta$  measurements were performed at room temperature using solutions of low ionic strength (i.e., Debye

length  $\kappa^{-1} \approx 0.8$  nm). Samples were prepared by adding 0.15 μg of COM crystals (seeds) to 3 mL of a saturated calcium oxalate solution (0.15 mM CaOx). Samples with modifiers were prepared by adding 50 μg/mL modifier to the solution, which was then stirred for 1 h prior to the measurement to allow sufficient time for adsorption of modifier on COM crystal surfaces. Each solution was transferred to a plastic cuvette equipped with a palladium electrode. The electrophoretic mobility was calculated using the Smoluchowski equation.

Time-resolved images of COM (010) surface growth were obtained by *in situ* atomic force microscopy (AFM) using a Digital Instruments Multimode IV (Santa Barbara, CA). AFM specimen disks (Ted Pella) were coated with a thin layer of thermally curable epoxy (MasterBond EP21AOLV), which was partially cured at 60 °C for 30 min. COM crystals were transferred to the AFM sample disk, which was heated in an oven at 60 °C for an additional hour to fully cure the epoxy. *In situ* measurements were performed with a solution of composition 0.18 mM CaCl<sub>2</sub> and 0.18 mM Na<sub>2</sub>C<sub>2</sub>O<sub>4</sub> (supersaturation ratio  $S = 3.8$ ), which was delivered to the AFM liquid sample cell using a dual syringe pump (CHEMYX, Fusion 200) with an in-line mixing configuration and a combined flow rate of 0.2 mL/min. The modifiers were introduced into the sample cell by their addition to the Na<sub>2</sub>C<sub>2</sub>O<sub>4</sub> solution. An Olympus TR800PSA cantilever (0.15 N/m spring constant) was used in contact mode with a scan rate of 8 Hz at 256 lines/scan.

Kinetic studies of COM crystallization were performed by measuring the depletion of free Ca<sup>2+</sup> ions using an Orion 9720BNWP ionplus calcium ion-selective electrode (ISE). A growth solution of molar composition 0.5 mM CaCl<sub>2</sub>/0.5 mM Na<sub>2</sub>C<sub>2</sub>O<sub>4</sub>/150 mM NaCl ( $S = 4.1$ ) was prepared at room temperature (see details in the Supporting Information). Modifiers were incorporated into the solution after the addition of CaCl<sub>2</sub> and prior to the addition of Na<sub>2</sub>C<sub>2</sub>O<sub>4</sub>. The electrode was placed in the solution immediately after adding Na<sub>2</sub>C<sub>2</sub>O<sub>4</sub>. The concentration of calcium was recorded for 1 h while the solution was continuously stirred at a rate of 1200 rpm (see Farmanesh et al. for details<sup>31</sup>). Prior to each ISE measurement, the electrode was calibrated with calcium standards prepared by first diluting a commercial calcium solution (0.1 M, Orion Ion Plus) in deionized water to three different concentrations (10<sup>-2</sup>, 10<sup>-3</sup>, and 10<sup>-4</sup> mol Ca<sup>2+</sup>/L) and then adding an ion strength adjuster (ISA, Thermo Scientific) in a 1:50 volume ratio of ISA-to-standard.

The pH of COM growth solutions was measured with an Orion 3-Star Plus pH benchtop meter and 8102BNUWP ROSS Ultra electrode (see Table S1 for pH values of each sample). A select number of modifiers tested in this study altered the pH upon their addition to the COM growth solution. Because pH affects supersaturation, which in turn influences COM growth kinetics, it was necessary to correct for any pH change by the addition of an appropriate amount of either NaOH or HCl stock solution to ensure that all kinetic studies were performed at approximately pH 6. Adjustment in pH was made prior to the addition of Na<sub>2</sub>C<sub>2</sub>O<sub>4</sub> for cases where the modifier produced more than a 0.2 change in pH. The concentration of HCl or NaOH needed to adjust solution pH never exceeded 0.02 mM, an amount that increased the Na<sup>+</sup> or Cl<sup>-</sup> ion concentration of growth solutions by ≤0.01% and had a negligible effect on COM growth rates.

## RESULTS AND DISCUSSION

**Physicochemical Factors Governing Modifier–Crystal Interactions.** In aqueous solutions, calcium ions dissociate from COM surfaces to generate a negatively charged crystalline interface (Figure 1). COM growth inhibitors rich in acidic groups (e.g., carboxylic acids) interact with Ca<sup>2+</sup> on the COM surface, mimicking oxalates via the formation of calcium bridges,  $(\text{COM})\text{COO}^- \cdots \text{Ca}^{2+} \cdots \text{OOC}(\text{modifier})$ , as shown in Figure 1 (dashed oval). Cationic groups of the modifier can potentially interact with negatively charged oxalate groups on a COM crystal surface to form a  $(\text{COM})\text{COO}^- \cdots \text{H}_3\text{N}(\text{modifier})$  bond (not shown in Figure 1). Ca<sup>2+</sup> ions in close proximity to COM surfaces may prevent basic groups of modifiers from directly

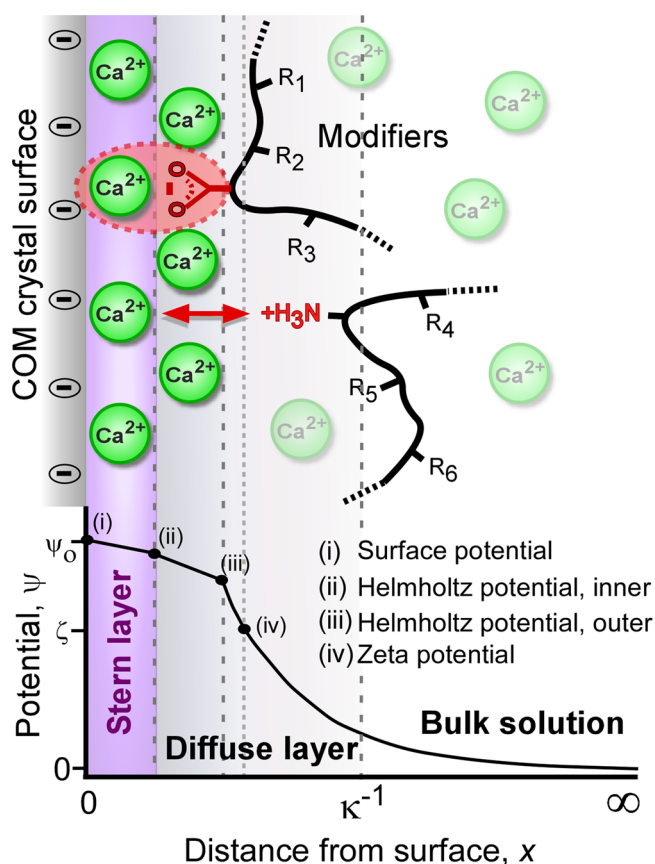


**Figure 1.** Conceptual depiction of modifier–COM interactions and the general trend of electrostatic potential decay as a function of distance from a COM crystal surface. Dissociation of  $\text{Ca}^{2+}$  ions in aqueous solution generates a negatively charged COM crystal interface. The Boltzmann equation predicts a higher concentration of counterions within the diffuse double layer ( $\kappa^{-1} \approx 0.8$  nm), which decays to the concentration of the bulk solution as  $x \rightarrow \infty$ . Modifiers with anionic functional moieties (e.g., side chains of Asp or Glu) bind to COM crystal surfaces via calcium bridges (dashed oval). Modifiers with cationic functional moieties (e.g., side chains of Lys) likely reside at distances farther from the surface due to electrostatic repulsion between the positively charged group and  $\text{Ca}^{2+}$  ions in the Stern layer (red arrow). The double layer consists of distinct regions, labeled i–iv. Here, we omit solvent molecules and additional ions ( $\text{Na}^+$ ,  $\text{H}^+$ ,  $\text{Cl}^-$ ,  $\text{OH}^-$ , and oxalate) for clarity.

binding to crystal surfaces due to electrostatic repulsion,  $\text{Ca}^{2+} \cdots \text{H}_3\text{N}_{(\text{modifier})}^+$ , as illustrated in Figure 1 (arrow). The fact that proteins are zwitterionic could lead to a variety of unique binding modes on crystal surfaces where the spatial sequencing (and proximal location) of binding groups within the primary amino acid sequence may determine their availability to interact with COM crystal surfaces. Protein secondary structure can dictate which of its segments are accessible for protein–crystal binding. Indeed, circular dichroism (CD) measurements of lactoferrin and lysozyme in aqueous solution reveal the presence of  $\alpha$ -helices and  $\beta$ -sheets (Figure S3); however, it is uncertain to what extent, if any, the structure is altered during protein adsorption on COM crystal surfaces in the presence of salts and ions. Without such knowledge, it is difficult to determine *a priori* which segments of the protein are accessible for protein–crystal interactions.

The schematic in Figure 1 presents a conceptual view of modifier–COM interactions on the basis of classical colloidal

theories. The diagram illustrates the general trend in electrostatic potential  $\psi$  in the double layer as a function of distance from a COM crystal surface. The distribution of ions in close proximity to the crystal interface is governed by the Boltzmann distribution,<sup>47</sup> which predicts an exponential decay in counterion concentration with increased distance from the charged surface, reaching concentrations equal to the bulk solution at distances beyond the diffuse double layer (i.e.,  $x > \kappa^{-1}$ ). In COM growth solutions, the concentrations of  $\text{Ca}^{2+}$ ,  $\text{Na}^+$ , and  $\text{H}^+$  ions are highest near crystal surfaces and reside within regions defined by an inner Helmholtz plane (or Stern layer) and an outer Helmholtz plane, which is shifted to farther distances from the crystal surface due to the hydrated shell surrounding the adsorbed cations. Analytical solutions of the Poisson–Boltzmann equation predict an exponential decay of  $\psi$  with increased distance from the charged interface. The triple layer theory, a surface complexation model that accounts for counterion hydration,<sup>48,49</sup> predicts an approximate linear decay of  $\psi$  in each Helmholtz layer (as illustrated in regions i–ii and ii–iii of Figure 1).

Modifiers that reside within the diffuse double layer can alter the net charge of the crystal. A common assumption is that surface potential  $\psi_0$  is approximately equal to zeta potential  $\zeta$ . The latter is measured at the plane of shear (Figure 1, iv). Here, we measured  $\zeta$  for COM crystals in the presence of three growth modifiers with varying isoelectric points (pI) spanning net negative to net positive charge. In the absence of modifier, COM crystals were found to have a negative  $\zeta$  ( $-16.1 \pm 0.9$  mV). As shown in Figure 2, the addition of lysozyme (pI > 11)<sup>50</sup> and lactoferrin (pI = 8.5)<sup>38</sup> shifted  $\zeta$  to positive values. For comparison, we analyzed the urinary protein transferrin (Tf), which has a lower isoelectric point (pI = 5.7–6.8).<sup>38,51,52</sup> The resulting  $\zeta$  for COM crystals in the presence of Tf is slightly negative. From this simple assay, it is evident that these

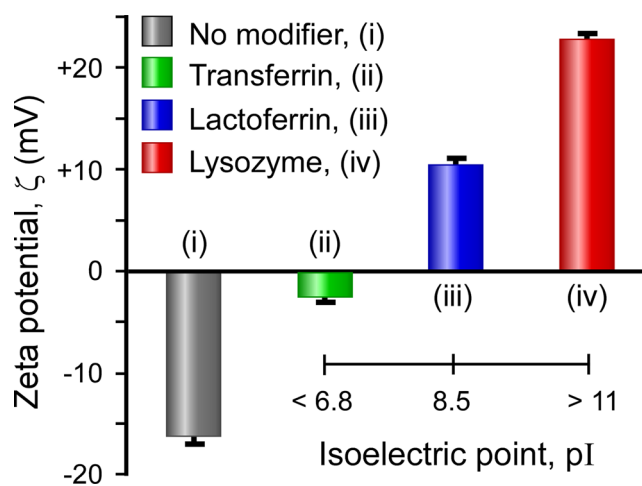


**Figure 2.** Zeta potential  $\zeta$  of COM crystals in aqueous solutions containing 50  $\mu\text{g}/\text{mL}$  of each modifier (transferrin, ii; lactoferrin, iii; and lysozyme, iv) and in the absence of modifier (control, i). Experiments were performed in saturated calcium oxalate solutions (0.15 mM CaOx, pH 6.1) containing 0.05  $\mu\text{g}/\text{mL}$  COM crystal seeds (see the Supporting Information for details). Measurements at room temperature produced slightly negative  $\zeta$  for transferrin and positive  $\zeta$  for lactoferrin and lysozyme. Data are the average of more than three measurements using separately prepared samples. Error bars equal 1 standard deviation.

three proteins reside within the diffuse double layer surrounding COM crystals.

**Kinetic Studies of COM Growth Modification.** We used an ion-selective electrode (ISE) to track the depletion of free  $\text{Ca}^{2+}$  ions in supersaturated solutions during crystal growth. The slope of ISE curves represents the kinetic rate of COM crystallization. These studies were performed in the presence of three classes of putative growth modifiers: amino acids (constituent units), polyamino acids (short-chain repeating units), and proteins. We first examined the effects of amino acids with acidic and basic side chains, selecting the most common constituents of urinary proteins that contribute to their anionic and cationic charges, respectively. The addition of amino acids to COM growth solutions resulted in an appreciable change in solution pH, which had a notable effect on the rate of COM growth (see the Supporting Information for additional details). In COM growth solutions, the carboxylic acid groups of acidic amino acids (Glu and Asp) are dissociated, and the amine groups of basic amino acids (Lys and Arg) are protonated. In order to maintain a constant pH, and hence constant calcium oxalate supersaturation (i.e., the driving force for COM crystallization),<sup>55</sup> the pH was adjusted using stock solutions of either HCl or NaOH. We avoided the use of buffers, such as HEPES or phosphates, which could potentially affect the rate of crystallization by adsorbing on COM surfaces and/or forming complexes with solute in growth solutions.

In order to better facilitate comparison of modifier efficacy, we report the results of ISE measurements as a relative growth rate (RGR) of COM crystallization

$$\text{RGR} = r_{\text{modifier}}/r_{\text{control}} \quad (1)$$

where  $r_i$  is the growth rate (ppm/min) measured as the slope of the ISE curve in the absence ( $r_{\text{control}}$ ) or presence ( $r_{\text{modifier}}$ ) of modifier. This parameter leads to a more facile identification of modifiers that behave as COM growth promoters (RGR > 1) or inhibitors (RGR < 1). A comparison of amino acids (Table 1) shows that anionic species inhibit COM growth by ca. 35%. Prior studies have reported that poly-L-aspartic acid (poly-D) is a more effective inhibitor than poly-L-glutamic acid (poly-E).<sup>54</sup> Our measurements did not reveal a significant difference between Asp and Glu amino acids, which is qualitatively

**Table 1. Comparison of COM Crystal Growth Modifiers**

growth modifiers <sup>a</sup>	$C_{\text{modifier}}$ ( $\mu\text{g/mL}$ )	RGR <sup>b</sup>
<b>Amino Acids</b>		
lysine (Lys, K)	80	0.93 $\pm$ 0.07
arginine (Arg, R)	80	1.06 $\pm$ 0.09
aspartic acid (Asp, D)	80	0.63 $\pm$ 0.10
glutamic acid (Glu, E)	80	0.68 $\pm$ 0.14
<b>Polyamino Acids</b>		
polylysine (poly-K)	20	1.03 $\pm$ 0.04
polyarginine (poly-R)	20	1.04 $\pm$ 0.03
polyaspartic acid (poly-D)	20	0.14 $\pm$ 0.08
polyglutamic acid (poly-E)	20	0.12 $\pm$ 0.09
<b>Proteins</b>		
transferrin (Tf)	80	0.87 $\pm$ 0.06
lactoferrin	80	1.08 $\pm$ 0.05
lysozyme	80	1.20 $\pm$ 0.05

<sup>a</sup>Solution with 0.5 mM CaOx: 150 mM NaCl ( $S = 4.1$ ) at pH 6.1, 25 °C, and with modifier concentration  $C_{\text{modifier}}$  ( $\mu\text{g/mL}$ ). <sup>b</sup>Relative growth rate (eq 1) from ISE data.

consistent with Fleming et al.,<sup>55</sup> who studied amino acid adsorption on COM crystals and reported that the equilibrium quantity of adsorbed Asp (0.071  $\mu\text{mol/m}^2$ ) is similar to that of Glu (0.067  $\mu\text{mol/m}^2$ ). Moreover, their study revealed a significantly lower quantity of adsorbed Lys and Arg on COM crystals (0.014 and 0.017  $\mu\text{mol/m}^2$ , respectively), which is consistent with our measurements of RGR  $\approx$  1 for COM growth in the presence of Lys and Arg (Table 1 and Figure S9).

Polyamino acids tend to be more potent modifiers than their corresponding amino acids.<sup>54</sup> For instance, the acidic polyamino acids poly-D and poly-E inhibit COM growth by ca. 90% (Table 1), i.e., 3-fold higher than that of D and E. Here, we tested two basic polyamino acids, polylysine (poly-K) and polyarginine (poly-R), to assess if the same trend holds true for cationic polymers. Interestingly, we observed very little change in the relative growth rate of COM in the presence of polycations (RGR  $\approx$  1, Table 1). This suggests that positively charged species do not strongly interact with COM surfaces, which could be attributed to the repulsive interactions between  $\text{Ca}^{2+}$  ions in the Stern layer and cationic moieties of modifiers in the double layer (see Figure 1).

Kinetic studies of COM crystallization in the presence of lactoferrin and lysozyme revealed that both cationic proteins are COM growth promoters, with the latter having a more pronounced effect on the accelerated rate of crystal growth (Table 1). This observation is opposite the effect of most anionic urinary proteins that behave as COM growth inhibitors. Indeed, COM growth is inhibited in the presence of transferrin, a common urinary protein with net negative charge. A systematic investigation of protein efficacy is presented in Figure 3, where we examined COM growth over a range of

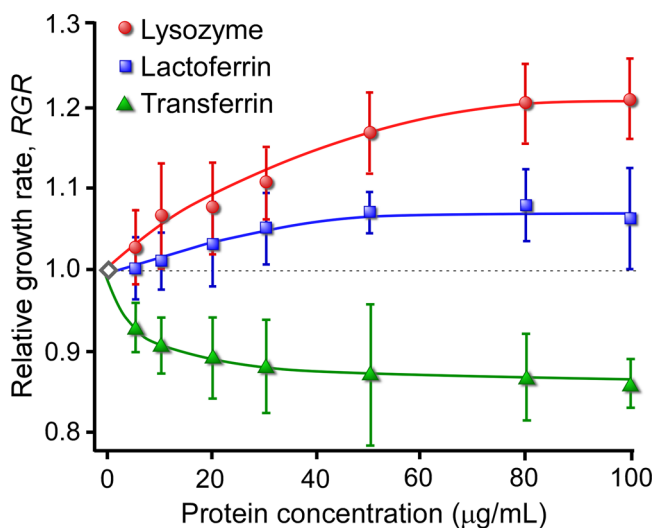


**Figure 3.** Relative growth rate (eq 1) of COM as a function of protein concentration. Data are the average of three or more separate ISE measurements. Error bars equal 2 standard deviations, solid lines are interpolated, and the dashed line signifies RGR = 1 (equal to the control).

protein concentrations. The curves in this figure exhibit a monotonic increase (for promoters) or decrease (for inhibitors) in RGR as a function of protein concentration. RGR values reach a plateau at some threshold concentration, beyond which further addition of the modifier has little added effect on the rate of COM crystallization.

ISE measurements of COM growth in the presence of transferrin revealed a maximum of 13% inhibition at a threshold concentration of ca. 30  $\mu\text{g/mL}$ ; for lactoferrin, we observed 8% promotion at ca. 50  $\mu\text{g/mL}$ ; and for lysozyme, we observed 20% promotion at ca. 80  $\mu\text{g/mL}$ . Inspection of the primary amino acid sequences of lysozyme (Figure S1) and lactoferrin (Figure S2) reveals that these proteins contain a high percentage of amino acids with basic side chains. One hypothesis that can be drawn from ISE measurements is that COM growth promotion increases with increase in protein pI. If we extend this line of thinking to anionic proteins, such as serum albumin<sup>30</sup> and OPN,<sup>56</sup> there is an apparent trend of decreasing relative growth rate with decreasing pI; however, the degree to which protein charge determines its role as a COM growth modifier is less apparent when considering a broader set of examples in the literature. For instance, proteins rich in basic amino acids, such as histone-lysine *N*-methyltransferase, inward rectifier K channel, and protein Wnt-2, are putative inhibitors of COM crystallization.<sup>41</sup> Conversely, there are proteins rich in acidic amino acids that reportedly act as COM growth promoters. Examples of the latter include ethanolamine-phosphate cytidyltransferase (pI = 6.4), Ras GTPase-activating-like protein (pI = 5.5), and macrophage-capping protein (pI = 5.8).<sup>57</sup>

Mechanisms of growth modification are derived from fundamental studies of classical crystallization involving layer-by-layer growth via ion/molecule addition. Growth inhibitors exhibit two principal modes of action: (i) step pinning, where the adsorption of a modifier on a crystal terrace impedes step advancement within the plane of adsorption, and (ii) modifier binding to steps, which frustrates solute attachment to advancing layers. The hypotheses proposed for the mechanism of growth promotion include (i) increased local supersaturation at crystal interfaces due to an enhanced attraction of solute molecules to the surface via solute-promoter interactions,<sup>58</sup> (ii) perturbation of hydration layers at the crystal surface as a result of promoter–crystal interactions, which can reduce the energy barrier for solute attachment,<sup>59</sup> and (iii) surface free energy arguments that suggest adsorbed promoters lower the edge energy of advancing layers on the crystal surface.<sup>60</sup> It is rarely reported that a modifier acts solely as a crystal growth promoter. A more common phenomenon is growth promotion at low modifier concentration and a transition to growth inhibition at higher modifier concentration. For example, Elhadj et al. identified anionic peptides that act as promoters of calcite ( $\text{CaCO}_3$ ) crystallization at low peptide concentration and that switch to growth inhibitors at higher peptide concentration (>0.1  $\mu\text{g/mL}$ ).<sup>59</sup> A similar trend was reported by Wasylenki et al., who showed that strontium switches from that of a growth promoter to a growth inhibitor at  $\sim 20 \mu\text{g/mL}$   $\text{Sr}^{2+}$ .<sup>33</sup> It has been suggested that the transition from promoter to inhibitor occurs once the modifier coverage on the crystal surface reaches a level that is sufficient to induce step pinning.<sup>33</sup> In contrast, lysozyme and lactoferrin act solely as crystal growth promoters irrespective of their concentration (i.e., within the 1–6  $\mu\text{M}$  range tested here). The ISE curves of promoters (Figure 3) exhibit Langmuir-like behavior, wherein the RGR value monotonically increases and plateaus once the adsorbed modifier has presumably reached equilibrium coverage on the crystal surface.

**Bulk Crystallization Studies.** We used optical microscopy to assess the influence of proteins on COM crystal habit, quantifying changes in the average dimensions of crystals within

the (100) plane and the thickness in the [100] direction. The COM aspect ratio (or  $c/b$  ratio) was measured as the relative ratio of [001] length to [010] width of the basal surface. Analyses of COM crystals grown in the presence of lysozyme (Figure 4A) and lactoferrin (Figure S5A) revealed a ca. 8%

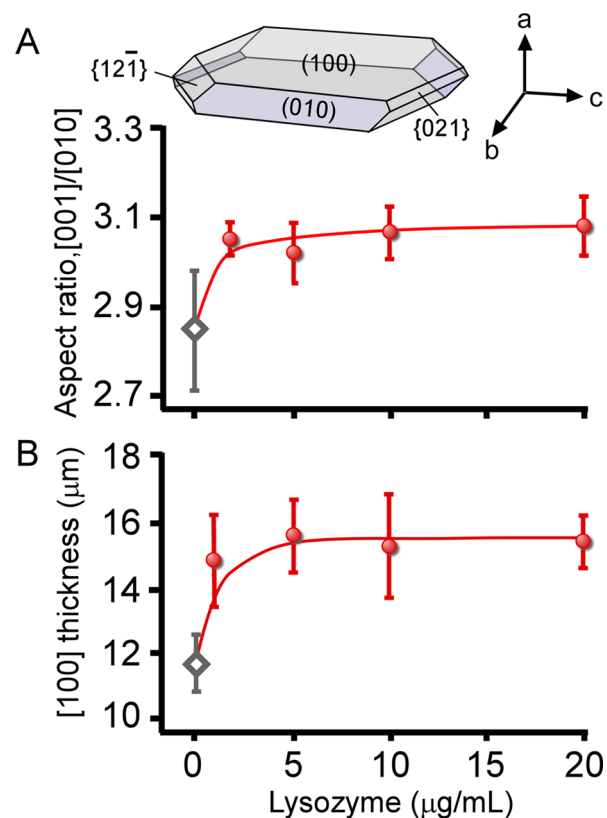


**Figure 4.** Influence of lysozyme on the bulk COM crystal habit. (A) Aspect ratio ( $c/b$ ) of the (100) basal plane measured as the ratio of [001] length to [010] width. The schematic highlights the indexed faces of COM crystals ( $P2_1/c$  space group).<sup>63</sup> (B) Changes in crystal [100] thickness with increasing lysozyme concentration. Data in panels A and B are the average of more than 150 and 50 crystals, respectively, that were measured from three separately prepared COM crystal batches. Open diamond symbols refer to the control. Error bars equal 2 standard deviations, and solid lines are interpolated.

increase in the COM crystal aspect ratio. The average dimensions of COM crystals along the [001] and [010] directions were not markedly influenced by the presence of either cationic protein (Figure S4); however, there was a noticeable increase in the [100] dimension of COM crystals. Lysozyme increased the thickness from 11 to 15  $\mu\text{m}$  (Figure 4B), and lactoferrin had a similar, albeit less pronounced, effect (ca. 8% increase, Figure S5B). The enhanced [100] dimension is qualitatively consistent with the Burton–Cabrerá–Frank (BCF) model (eq 2). COM crystals grow via a spiral dislocation mechanism. The BCF model predicts the rate of spiral growth normal to the (100) crystal face,  $G_{[100]}$ ,

$$G_{[100]} = \frac{(v_i)_{hkl} h_{hkl}}{(y_i)_{hkl}} = \frac{h}{\tau} \quad (2)$$

where steps with index ( $hkl$ ) and height  $h$  advance along the (100) plane with a characteristic time of spiral rotation  $\tau$ . The latter equals the ratio of interstep distance  $y_i$  to the velocity of step advancement  $v_i$ .<sup>61,62</sup> As we will discuss in the following

section, AFM measurements of COM surface growth reveal that lysozyme increases the rate of step advancement, thereby reducing  $\tau$  and increasing  $G_{[100]}$ . This can explain why larger COM [100] dimensions are observed in bulk crystallization studies.

The increased crystal aspect ratio can be attributed to the preferential interaction of lysozyme with COM {12 $\bar{1}$ } and/or {021} surfaces. Modifiers interacting with the apical surfaces promote growth along the  $c$  direction. Interestingly, bulk crystallization studies (Figure 4) reveal that the changes in COM crystal habit occur at low protein concentration (ca. 1  $\mu\text{g}/\text{mL}$ ), with no observable variation in crystal size and morphology at modifier concentrations as high as 100  $\mu\text{g}/\text{mL}$ . ISE data in Figure 3 reveal that growth promotion at 1  $\mu\text{g}/\text{mL}$  modifier is marginal, which is qualitatively consistent with a scanning confocal microscopy study by Grohe et al., who examined lysozyme–COM interactions using Alexa Fluor 488 fluorescently labeled lysozyme (at 1  $\mu\text{g}/\text{mL}$ ) and reported no detectable adsorption on COM crystals.<sup>42</sup> This seems to suggest that lysozyme–crystal interactions are weak, particularly in relation to growth inhibitors in the literature (e.g., OPN), which can have a substantial effect on COM crystal morphology and growth rate at low modifier concentration.

#### *In Situ* AFM Measurements of COM Surface Growth.

We used *in situ* AFM to elucidate the effect of promoters on the growth of COM (010) surfaces at a microscopic level, focusing solely on lysozyme (the more effective promoter). AFM has proven to be a valuable tool for investigating growth kinetics at near molecular resolution.<sup>9,64,65</sup> Here, we used this technique to collect time-resolved images of step advancement in supersaturated CaOx solutions ( $S = 3.8$ ) either in the absence or presence of lysozyme. COM (010) surfaces are composed of hillocks (Figure 5A) expressed by parallelogram-shaped layers

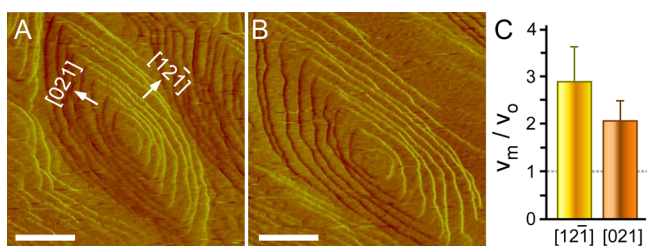


**Figure 5.** *In situ* AFM measurements of hillock growth on the COM (010) face in a supersaturated CaOx solution ( $S = 3.8$ ). Deflection mode images of a hillock growing in the absence of modifier (A) and in the presence of 2.5  $\mu\text{g}/\text{mL}$  lysozyme (B). Time-elapsed images of growth are provided as a movie in the Supporting Information. (C) Comparison of the relative step velocity,  $v_m/v_0$ , along the [12 $\bar{1}$ ] and [021] directions. The dashed line refers to the velocity of the control. The scale bars in panels A and B equal 500 nm.

with {12 $\bar{1}$ } and {021} steps. It is evident from *in situ* AFM studies that lysozyme induced an elongation of hillock morphology (Figure 5B). We quantitatively analyzed successive AFM images to calculate step velocities  $v_{(hkl)}$ . Results are reported as the relative step velocity  $v_m/v_0$ , where  $v_m$  and  $v_0$  are measured in the presence and absence of modifier, respectively, and  $v_m/v_0 > 1$  signifies accelerated step growth. As shown in Figure 5C, introduction of 2.5  $\mu\text{g}/\text{mL}$  lysozyme in the COM growth solution preferentially increases the rate of growth along the [12 $\bar{1}$ ] direction by nearly a factor of 3. Lysozyme also accelerates the rate of growth along the [021] direction by a

factor of 2. The modifier produced an approximate 47% increase in the interstep distance  $y_{[021]}$ , but it had much less effect on  $y_{[12\bar{1}]}$ . *In situ* AFM measurements at higher lysozyme concentration (5  $\mu\text{g}/\text{mL}$ ) revealed no additional change in hillock morphology (Figure S10) and did not result in surface roughening, a phenomenon that is characteristic of growth inhibition at high modifier concentrations.<sup>21,31</sup> The promotion of step velocity along the [021] and [12 $\bar{1}$ ] directions is qualitatively consistent with the increased RGR (Figure 3) and the increased  $c/b$  aspect ratio (Figure 4) of COM crystals observed in ISE and bulk crystallization studies, respectively.

**Peptides Derived from Lysozyme.** A common attribute of lactoferrin and lysozyme is their relatively large percentage of basic amino acids, which appear to be grouped in close proximity to each other within the native primary sequence of these proteins. It is interesting to note that among more than 1500 proteins identified by Righetti et al.,<sup>50</sup> lysozyme is one of two proteins with  $\text{pI} > 11$ , whereas less than 4% have  $\text{pI}$  equal to or greater than that of lactoferrin. Therefore, it could be postulated that protein segments rich in positively charged moieties are primarily responsible for COM growth promotion. In order to test this hypothesis, we synthesized 12 peptides never before studied that collectively span the entire primary amino acid sequence of lysozyme (Table 2), and we then tested

**Table 2. Peptides Derived from Contiguous Segments of Lysozyme**

Name	Position	Peptide sequences <sup>a</sup>	$\text{pI}$ <sup>b</sup>
L1	1 - 20	KVFGRC <b>E</b> LAAAM <b>K</b> RHGLDNY	9.20
L2	11 - 30	AM <b>K</b> RHGLDNY <b>R</b> GYSLG <b>N</b> WVC	9.20
L3	21 - 40	<b>R</b> GYSLG <b>N</b> WVCA <b>A</b> K <b>F</b> ES <b>N</b> FNT	8.20
L4	31 - 50	<b>A</b> A <b>K</b> <b>F</b> ES <b>N</b> FNT <b>Q</b> TT <b>N</b> R <b>N</b> TDGS	4.56
L5	41 - 60	QTT <b>N</b> R <b>N</b> TD <b>G</b> ST <b>D</b> Y <b>G</b> ILQ <b>N</b> IS	3.93
L6	51 - 70	<b>T</b> D <b>Y</b> G <b>I</b> L <b>Q</b> N <b>I</b> S <b>R</b> W <b>C</b> <b>N</b> D <b>G</b> R <b>T</b> P	5.62
L7	61 - 80	<b>R</b> W <b>W</b> C <b>N</b> D <b>G</b> R <b>T</b> P <b>G</b> S <b>R</b> N <b>L</b> C <b>N</b> I <b>P</b> C	8.73
L8	71 - 90	G <b>S</b> R <b>N</b> L <b>C</b> N <b>I</b> P <b>C</b> S <b>A</b> L <b>L</b> S <b>S</b> D <b>I</b> T <b>A</b>	5.82
L9	81 - 100	S <b>A</b> L <b>L</b> S <b>S</b> D <b>I</b> T <b>A</b> S <b>N</b> V <b>C</b> A <b>K</b> K <b>I</b> V <b>S</b>	7.92
L10	91 - 110	S <b>N</b> V <b>C</b> A <b>K</b> K <b>I</b> V <b>S</b> D <b>G</b> N <b>G</b> M <b>N</b> A <b>W</b> V <b>A</b>	5.68
L11	101 - 120	<b>D</b> G <b>N</b> G <b>M</b> N <b>A</b> W <b>V</b> A <b>W</b> R <b>N</b> R <b>C</b> K <b>G</b> T <b>D</b> V	6.03
L12	111 - 129	<b>W</b> R <b>N</b> R <b>C</b> K <b>G</b> T <b>D</b> V <b>Q</b> A <b>W</b> I <b>R</b> G <b>R</b> L	10.72

<sup>a</sup>Anionic amino with basic (green) and acidic (red) side groups.  
<sup>b</sup>Theoretical  $\text{pI}$  (ExPASy Bioinformatics Resource Portal).<sup>66</sup>

for segments that accelerated the rate of COM growth. Each peptide contains 20 consecutive amino acids generated by shifting the position of the first amino acid in intervals of 10. For example, the first peptide (labeled L1) contains amino acids located in positions 1–20, L2 contains positions 11–30, L3 contains positions 21–40, and so forth. Because lysozyme is composed of 129 amino acids, the final peptide (L12) is a 19-mer sequence. As shown in Table 2, lysozyme peptides exhibit a range of  $\text{pI}$  and are composed of disparate quantities of amino acids with either basic or acidic side chains (labeled as green or red, respectively).

The effects of peptides L1–L12 on the RGR of COM crystallization were quantitatively compared at 50  $\mu\text{g}/\text{mL}$  peptide (Figure 6). The results are subdivided into three categories: RGR  $> 1$  (promotion), RGR  $< 1$  (inhibition), and RGR  $\approx 1$  (negligible effect, dashed line). Interestingly, we observed a distribution of promoters and inhibitors with RGR values ranging from 0.85 to 1.1. To our knowledge, such behavior has not been reported in the literature for crystal

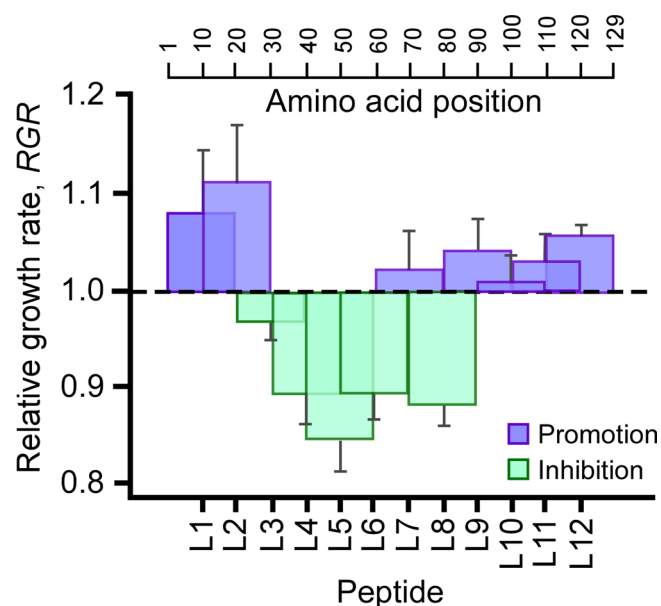


**Figure 6.** Relative growth rate (RGR, eq 1) in the presence of 50  $\mu\text{g}/\text{mL}$  of each lysozyme peptide listed in Table 2. Green and purple bars refer to COM growth inhibition ( $\text{RGR} < 1$ ) and promotion ( $\text{RGR} > 1$ ), respectively. Each histogram is a single peptide (lower  $x$  axis) plotted with a width corresponding to the position of amino acids in lysozyme (upper  $x$  axis). The histograms overlap to illustrate the 10-mer segments shared among peptides (see Table 2). Data are the average of more than three ISE measurements. Error bars equal 1 standard deviation.

growth modifiers. It is far more common to find studies where only specific segments of proteins (e.g., those with the highest density of acidic moieties) are hand-selected and are shown to possess varying efficacy as inhibitors. An analysis of the entire protein sequence is less common, possibly due to the prohibitively large size of most proteins. In dissecting the sequence of lysozyme, we observed a dichotomy whereby discrete subdomains display completely opposite effects as crystal modifiers. Lysozyme peptides that exhibited the strongest inhibitory effects occupy positions within the middle of the amino acid sequence. It is reasonable to suggest that a fraction of these segments are not presented on the exterior of the protein and hence may be sterically restricted from participating in lysozyme–COM interactions. Conversely, the segments identified as growth promoters are located on either end of the protein sequence; therefore, it is likely that these portions of the protein are more readily available to interact with COM crystal surfaces. The most effective growth promoters (L1, L2, and L12) resulted in a ca. 10% increase in COM growth rate, which is comparable to that of lysozyme at the same concentration.

There is an apparent correlation between the RGR of COM crystallization and peptide pI (Figure 7A). Peptides rich in anionic side chains (i.e., low pI) are the most effective inhibitors of COM growth; these include L4, L5, L6, and L8. Conversely, peptides rich in cationic side chains (i.e., high pI) are the most effective promoters of COM growth; these include L1, L2, and L12. The net charge of COM modifiers is often invoked in the literature as a descriptor of their efficacy. Similar corollaries have been postulated for calcium phosphate crystallization. For instance, Azzopardi et al. examined the binding of OPN peptides to hydroxyapatite crystals by molecular modeling and

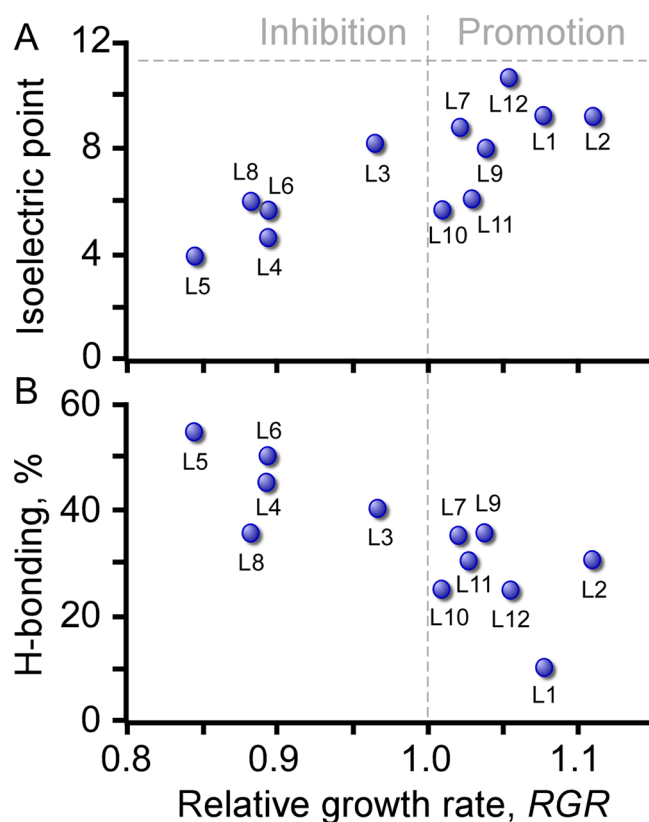


**Figure 7.** General correlations for the RGR of COM in the presence of lysozyme peptides, plotted as a function of peptide isoelectric point (A) and percentage of H-bonding side chains (B). Calculations of the latter exclude amino acids with charged side chains (Asp, Glu, Lys, Arg, His) and include only the following amino acids: Asn, Gln, Ser, Thr, Trp, and Tyr. Linear regression of data in panels A and B yields  $R^2 \approx 0.65$ .

kinetic studies, in which they report a linear increase in the strength of peptide adsorption (and potency) with decreasing pI.<sup>67</sup> In our study, however, there are examples that contradict the overarching correlation in Figure 7A. For instance, a comparison of peptides with pI in the range of 5.6–6.0 reveals that L6 and L8 are inhibitors of COM growth, whereas L10 and L11 are mild promoters. As such, *a priori* assessment of modifiers on the basis of pI is merely one metric for estimating their efficacy.

Closer inspection of ISE data suggests that the percentage of H-bonding side chains on peptides L1–L12 can be used as an additional descriptor of COM growth modification. For instance, we observe an apparent correlation between the relative growth rate of COM crystals and the percentage of H-bonding residues in each lysozyme peptide (Figure 7B). For this analysis, the calculation of percent H-bonding residues excludes basic and acidic side chains and only accounts for amino acids that possess alcohol and amine moieties: L-asparagine (Asn), L-glutamine (Gln), L-serine (Ser), L-threonine (Thr), L-tryptophan (Trp), and L-tyrosine (Tyr). The most effective lysozyme peptide inhibitors (L4, L5, and L6) are composed of more than 40% H-bonding amino acids, whereas the most effective promoters (L1, L2, and L12) contain less than 30% H-bonding amino acids. Other groups have made similar comparisons, reporting that proteins<sup>42</sup> and peptides<sup>65</sup> with a higher content of hydrophilic amino acids are more potent COM growth inhibitors. There are clearly outliers in Figure 7B,

which suggests that the effect of a modifier cannot be solely predetermined on the basis of any single descriptor; however, trends in Figure 7 do offer some general guidelines for approximating whether a peptide is more likely to act as an inhibitor or as a promoter of COM crystallization.

The segments of lysozyme responsible for COM growth promotion were further refined by synthesizing 10-mer peptides corresponding to overlapping sequences in Table 2 with the highest RGR values. The two most effective promoters are L1 and L2, which share the overlapping sequence AMKRHGLDNY (referred to as L13 in Table 3). This peptide

**Table 3. Peptides Derived from Sequences of COM Growth Promoters**

Name	Position	Peptide sequences <sup>a</sup>	pI <sup>b</sup>	HB (%) <sup>c</sup>	RGR <sup>d</sup>
L13	11 - 20	AM <b>KRH</b> GLDNY	8.64	20	1.06 ± 0.04
L13G		GG <b>KRH</b> GGDGG	8.75	0	1.05 ± 0.04
L14	111 - 120	WR <b>NRCK</b> GTDV	9.50	30	1.05 ± 0.04
L14G		GR <b>GRK</b> GGDGG	10.84	0	1.06 ± 0.04

<sup>a</sup>Anionic amino acids with basic (green) and acidic (red) side chains.

<sup>b</sup>Theoretical pI (ExPASy Bioinformatics Resource Portal).<sup>13</sup> <sup>c</sup>Percentage of H-bonding (HB) amino acids (N, W, Q, T, Y). <sup>d</sup>Relative growth rate (eq 1) using the same conditions as in Table 1.

contains a consecutive sequence of three amino acids with basic side chains, KRH, and a single acidic amino acid (Asp, D). We selected a second set of peptide growth promoters, L11 and L12, and examined their overlapping 10-mer sequence WRNRCKGTDV (L14 in Table 3). This peptide is similarly composed of three basic amino acids and a single acidic amino acid; however, the former are spatially separated in the sequence RXRXK (where X is a spacer). As listed in Table 3, COM growth in the presence of peptides L13 and L14 resulted in a ca. 5% increase in crystal growth rate, which is comparable to that of their parent peptides (within experimental error). One question posed in this study was whether COM growth promotion is attributed to the spatial sequence of charged side chains of the peptides (i.e., *binder* moieties that promote peptide–crystal interactions) and is independent of all other amino acids (so-called *spacer* moieties). To this end, we performed L-glycine (Gly) substitution of peptides L13 and L14 to replace all amino acids except those with acidic (D, E) and basic (K, H, R) side chains. Peptides synthesized with Gly-substitution are referred to as L13G and L14G, respectively.

ISE measurements showed that L13 and L13G have identical RGR values. Likewise, L14 and L14G have similar effects on COM growth. This suggests that the charged groups in the peptide sequence are predominantly responsible for COM growth promotion. One unexpected result of this study was that the removal of 20–30% of the H-binding amino acids due to Gly substitution (Table 3) had no apparent effect on peptide efficacy. On the basis of the trend reported in Figure 7B, it was anticipated that the removal of H-binding residues would result in a more effective promoter, which was not observed in this case.

Peptides identified as promoters in Tables 2 and 3 possess a larger percentage of basic residues; however, each has at least one acidic amino acid. The spatial sequence of amino acids in the peptide appears to govern its efficacy, i.e., basic groups in the most effective promoters are located in close proximity to each other. It is evident that some degree of anionic charge is essential to promote COM crystal growth. For instance, we

showed that the effects of purely cationic amino acids and polyamino acids on COM crystallization were negligible (Table 1). One hypothesis, based on the idealized modifier–crystal interactions depicted in Figure 1, is that the anionic side chains are necessary to increase the strength of peptide–COM crystal interactions (perhaps to more closely “anchor” peptides to the crystal surface). It is reasonable to suggest that the basic side chains are responsible for growth promotion; however, a molecular level understanding of peptide action cannot be gleaned from the studies presented here. This level of detail requires molecular modeling to assess entropic effects (i.e., hydration of COM interfaces), to identify the structure(s) of adsorbed peptides, and to elucidate the mechanism(s) of peptide binding to COM surfaces. Modeling of growth promoter peptides identified in this study is ongoing (the results will be reported at a later date).

## CONCLUSIONS

In summary, we identified two proteins that promote COM growth by accelerating the rate of layer advancement on crystal surfaces. A systematic analysis of lysozyme was performed where its entire amino acid sequence was subdivided into contiguous peptides (10–20 amino acids in length). This study revealed that the sequences responsible for growth promotion are rich in basic side chains. We observed that lysozyme is composed of subdomains that function as either promoters or inhibitors of COM growth. Peptides identified as inhibitors are located in the middle of the primary amino acid sequence, which suggests that steric restrictions may limit their interaction with COM surfaces. Conversely, it is reasonable to expect that peptide promoters (located on either terminus) exhibit fewer steric restrictions.

There are few prior examples of crystal growth promoters. Among those identified in the literature, a common phenomenon is that modifiers operate as crystal growth promoters only at low modifier concentration and switch to growth inhibitors at higher concentration. Our findings seem to suggest that lysozyme and lactoferrin operate by a different mechanism. Indeed, the characteristic ISE profile of crystal growth promoters closely resembles the Langmuir-like behavior of COM growth inhibitors.<sup>31</sup> What is currently lacking from this analysis is a molecular-level description of modifier–crystal interactions that identifies the exact mechanism of COM growth promotion. Defining an inclusive set of heuristic guidelines capable of predicting the role of growth modifiers is challenging, yet general trends are proposed in this study to estimate modifier efficacy on the basis of its physicochemical properties.

The observation that lysozyme and lactoferrin promote COM crystallization may reflect a more universal role of these proteins in biomineralization. Results of this study are qualitatively consistent with observations that cationic proteins are observed in three types of pathological stones (kidney, pancreas, and prostate). Although it is not feasible to draw definitive conclusions of *in vivo* processes from *in vitro* assays, we can suggest only that lysozyme and lactoferrin may play an active role in stone pathogenesis. In a broader context, the pathway of crystal growth promotion may allude to a more widespread mechanism of biogenic mineral formation (e.g., bone or exoskeletal structures). From a practical standpoint, the design of growth promoters offers a potential route to reduce the time of commercial crystallization, and, in certain applications, growth promoters may prove to be useful for



tailoring crystal size and/or habit. The fact that such effects can be achieved with small peptides (i.e., constitutive segments of larger proteins) is advantageous for the design of biomimetic modifiers for applications that span pharmaceuticals to materials synthesis.

## ■ ASSOCIATED CONTENT

### ● Supporting Information

Experimental materials and methods; protein structures and amino acid sequences; CD spectra; pH correction of COM growth solutions; COM bulk crystallization at varying concentrations of lactoferrin; ISE measurements of COM crystallization in the presence of amino acids; AFM image of COM (010) surface growth at high lysozyme concentration; and movie S1 (*in situ* AFM). This material is available free of charge via the Internet at <http://pubs.acs.org>.

## ■ AUTHOR INFORMATION

### Corresponding Author

[jrimer@central.uh.edu](mailto:jrimer@central.uh.edu)

### Notes

The authors declare no competing financial interest.

## ■ ACKNOWLEDGMENTS

We acknowledge financial support from the National Science Foundation (DMR award nos. 1207441 and 1207411) and the Welch Foundation (E-1794).

## ■ REFERENCES

- (1) De Yoreo, J. J.; Qiu, S. R.; Hoyer, J. R. *Am. J. Physiol.: Renal Physiol.* **2006**, *291*, F1123.
- (2) Oner, M.; Dogan, O.; Oner, G. *J. Cryst. Growth* **1998**, *186*, 427.
- (3) Suzuki, M.; Saruwatari, K.; Kogure, T.; Yamamoto, Y.; Nishimura, T.; Kato, T.; Nagasawa, H. *Science* **2009**, *325*, 1388.
- (4) Gower, L. B. *Chem. Rev.* **2008**, *108*, 4551.
- (5) Ndao, M.; Keene, E.; Amos, F. F.; Rewari, G.; Ponce, C. B.; Estroff, L.; Evans, J. S. *Biomacromolecules* **2010**, *11*, 2539.
- (6) Nancollas, G. H.; Tang, R.; Phipps, R. J.; Henneman, Z.; Gulde, S.; Wu, W.; Mangood, A.; Russell, R. G. G.; Ebetino, F. H. *Bone* **2006**, *38*, 617.
- (7) East, C. P.; Wallace, A. D.; Al-Hamzah, A.; Doherty, W. O. S.; Fellows, C. M. *J. Appl. Polym. Sci.* **2010**, *115*, 2127.
- (8) Taller, A.; Grohe, B.; Rogers, K. A.; Goldberg, H. A.; Hunter, G. K. *Biophys. J.* **2007**, *93*, 1768.
- (9) Cho, K. R.; Salter, E. A.; De Yoreo, J. J.; Wierzbicki, A.; Elhadji, S.; Huang, Y.; Qiu, S. R. *CrystEngComm* **2013**, *15*, 54.
- (10) Shirane, Y.; Kurokawa, Y.; Miyashita, S.; Komatsu, H.; Kagawa, S. *Urol. Res.* **1999**, *27*, 426.
- (11) Thanasekaran, P.; Liu, C. M.; Cho, J. F.; Lu, K. L. *Inorg. Chem. Commun.* **2012**, *17*, 84.
- (12) Aihara, K.; Byer, K. J.; Khan, S. R. *Kidney Int.* **2003**, *64*, 1283.
- (13) Grases, F.; Isern, B.; Perello, J.; Costa-Bauza, A. *BJU Int.* **2004**, *94*, 177.
- (14) Hess, B. *Urol. Res.* **1992**, *20*, 83.
- (15) Assimos, D. *J. Urol.* **2011**, *186*, 576.
- (16) Carvalho, M.; Mulinari, R. A.; Nakagawa, Y. *Braz. J. Med. Biol. Res.* **2002**, *35*, 1165.
- (17) Ebrahimpour, A.; Perez, L.; Nancollas, G. H. *Langmuir* **1991**, *7*, 577.
- (18) Jiang, Z. R.; Asplin, J. R.; Evan, A. P.; Rajendran, V. M.; Velazquez, H.; Nottoli, T. P.; Binder, H. J.; Aronson, P. S. *Nat. Genet.* **2006**, *38*, 474.
- (19) Selvam, R.; Kalaiselvi, P. *Urol. Res.* **2003**, *31*, 242.
- (20) Jung, T.; Sheng, X. X.; Choi, C. K.; Kim, W. S.; Wesson, J. A.; Ward, M. D. *Langmuir* **2004**, *20*, 8587.
- (21) Qiu, S. R.; Wierzbicki, A.; Orme, C. A.; Cody, A. M.; Hoyer, J. R.; Nancollas, G. H.; Zepeda, S.; De Yoreo, J. J. *Proc. Natl. Acad. Sci. U.S.A.* **2004**, *101*, 1811.
- (22) Sheng, X. X.; Ward, M. D.; Wesson, J. A. *J. Am. Chem. Soc.* **2003**, *125*, 2854.
- (23) Thurgood, L. A.; Cook, A. F.; Sorensen, E. S.; Ryall, R. L. *Urol. Res.* **2010**, *38*, 357.
- (24) Wesson, J. A.; Johnson, R. J.; Mazzali, M.; Beshensky, A. M.; Stietz, S.; Giachelli, C.; Liaw, L.; Alpers, C. E.; Couser, W. G.; Kleinman, J. G.; Hughes, J. *J. Am. Vet. Med. Assoc.* **2003**, *14*, 139.
- (25) Grohe, B.; O'Young, J.; Ionescu, D. A.; Lajoie, G.; Rogers, K. A.; Karttunen, M.; Goldberg, H. A.; Hunter, G. K. *J. Am. Chem. Soc.* **2007**, *129*, 14946.
- (26) Hoyer, J. R.; Asplin, J. R.; Otvos, L. *Kidney Int.* **2001**, *60*, 77.
- (27) Wang, L. J.; Guan, X. Y.; Tang, R. K.; Hoyer, J. R.; Wierzbicki, A.; De Yoreo, J. J.; Nancollas, G. H. *J. Phys. Chem. B* **2008**, *112*, 9151.
- (28) Qiu, S. R.; Wierzbicki, A.; Salter, E. A.; Zepeda, S.; Orme, C. A.; Hoyer, J. R.; Nancollas, G. H.; Cody, A. M.; De Yoreo, J. J. *J. Am. Chem. Soc.* **2005**, *127*, 9036.
- (29) Weaver, M. L.; Qiu, S. R.; Hoyer, J. R.; Casey, W. H.; Nancollas, G. H.; De Yoreo, J. J. *ChemPhysChem* **2006**, *7*, 2081.
- (30) Ryall, R. L.; Harnett, R. M.; Hibberd, C. M.; Edyvane, K. A.; Marshall, V. R. *Urol. Res.* **1991**, *19*, 181.
- (31) Farmanesh, S.; Ramamoorthy, S.; Chung, J.; Asplin, J. R.; Karande, P.; Rimer, J. D. *J. Am. Chem. Soc.* **2014**, *136*, 367.
- (32) Clark, R. H.; Campbell, A. A.; Klumb, L. A.; Long, C. J.; Stayton, P. S. *Calcif. Tissue Int.* **1999**, *64*, 516.
- (33) Wasylenki, L. E.; Dove, P. M.; Wilson, D. S.; De Yoreo, J. J. *Geochim. Cosmochim. Acta* **2005**, *69*, 3017.
- (34) Elhadji, S.; Salter, E. A.; Wierzbicki, A.; De Yoreo, J. J.; Han, N.; Dove, P. M. *Cryst. Growth Des.* **2006**, *6*, 197.
- (35) Ouyang, H. M.; Deng, S. P.; Zhong, J. P.; Tieke, B.; Yu, S. H. *J. Cryst. Growth* **2004**, *270*, 646.
- (36) Khan, S. R. *Urol. Int.* **1997**, *59*, 59.
- (37) Lominadze, G.; Powell, D. W.; Luerman, G. C.; Link, A. J.; Ward, R. A.; McLeish, K. R. *Mol. Cell. Proteomics* **2005**, *4*, 1503.
- (38) Canales, B. K.; Anderson, L.; Higgins, L.; Slaton, J.; Roberts, K. P.; Liu, N. T.; Monga, M. J. *Endourol.* **2008**, *22*, 1161.
- (39) Chen, W. C.; Lai, C. C.; Tsai, Y. H.; Lin, W. Y.; Tsai, F. J. *J. Clin. Lab. Anal.* **2008**, *22*, 77.
- (40) Mushtaq, S.; Siddiqui, A. A.; Naqvi, Z. A.; Rattani, A.; Talati, J.; Palmberg, C.; Shafqat, J. *Clin. Chim. Acta* **2007**, *384*, 41.
- (41) Aggarwal, K. P.; Tandon, S.; Naik, P. K.; Singh, S. K.; Tandon, C. *Clin. Chim. Acta* **2013**, *415*, 181.
- (42) Grohe, B.; Taller, A.; Vincent, P. L.; Tieu, L. D.; Rogers, K. A.; Heiss, A.; Sorensen, E. S.; Mittler, S.; Goldberg, H. A.; Hunter, G. K. *Langmuir* **2009**, *25*, 11635.
- (43) Sfanos, K. S.; Wilson, B. A.; De Marzo, A. M.; Isaacs, W. B. *Proc. Natl. Acad. Sci. U.S.A.* **2009**, *106*, 3443.
- (44) Jin, C. X.; Naruse, S.; Kitagawa, M.; Ishiguro, H.; Kondo, T.; Hayakawa, S.; Hayakawa, T. *JOP* **2002**, *3*, 54.
- (45) Houser, M. T. *Clin. Chem.* **1983**, *29*, 1488.
- (46) Farmanesh, S.; Chung, J.; Chandra, D.; Sosa, R. D.; Karande, P.; Rimer, J. D. *J. Cryst. Growth* **2013**, *373*, 13.
- (47) Hiemenz, P. C.; Rajagopalan, R. *Principles of Colloid and Surface Chemistry*, 3rd ed.; Marcel Dekker: New York, 1997.
- (48) Westall, J.; Hohl, H. *Adv. Colloid Interface Sci.* **1980**, *12*, 265.
- (49) Davis, J. A.; James, R. O.; Leckie, J. O. *J. Colloid Interface Sci.* **1978**, *63*, 480.
- (50) Righetti, P. G.; Tudor, G.; Ek, K. *J. Chromatogr. A* **1981**, *220*, 115.
- (51) Legendre, J. M.; Moineau, M. P.; Menez, J. F.; Turzo, A. *Pathol. Biol.* **1985**, *33*, 741.
- (52) Beving, H.; Malmgren, R.; Petren, S.; Vesterberg, O. *J. Soc. Occup. Med.* **1991**, *41*, 102.
- (53) De Yoreo, J. J.; Vekilov, P. G. In *Biomimetalization*; Dove, P. M., DeYoreo, J. J., Weiner, S., Eds.; **2003**; Vol. 54, p 57.
- (54) Guo, S. W.; Ward, M. D.; Wesson, J. A. *Langmuir* **2002**, *18*, 4284.

(55) Fleming, D. E.; van Bronswijk, W.; Ryall, R. L. *Clin. Sci.* **2001**, *101*, 159.

(56) Wang, L. J.; Zhang, W.; Qiu, S. R.; Zachowicz, W. J.; Guan, X. Y.; Tang, R. K.; Hoyer, J. R.; De Yoreo, J. J.; Nancollas, G. H. *J. Cryst. Growth* **2006**, *291*, 160.

(57) Aggarwal, K. P.; Tandon, S.; Naik, P. K.; Singh, S. K.; Tandon, C. *PLoS One* **2013**, *8*, e69916.

(58) Fu, G.; Qiu, S. R.; Orme, C. A.; Morse, D. E.; De Yoreo, J. J. *Adv. Mater.* **2005**, *17*, 2678.

(59) Elhadj, S.; De Yoreo, J. J.; Hoyer, J. R.; Dove, P. M. *Proc. Natl. Acad. Sci. U.S.A.* **2006**, *103*, 19237.

(60) Madsen, H. E. L. *J. Cryst. Growth* **2008**, *310*, 2602.

(61) Lovette, M. A.; Browning, A. R.; Griffin, D. W.; Sizemore, J. P.; Snyder, R. C.; Doherty, M. F. *Ind. Eng. Chem. Res.* **2008**, *47*, 9812.

(62) Snyder, R. C.; Doherty, M. F. *Proc. R. Soc. London, Ser. A* **2009**, *465*, 1145.

(63) Tazzoli, V.; Domeneghetti, C. *Am. Mineral.* **1980**, *65*, 327.

(64) Rimer, J. D.; An, Z. H.; Zhu, Z. N.; Lee, M. H.; Goldfarb, D. S.; Wesson, J. A.; Ward, M. D. *Science* **2010**, *330*, 337.

(65) Wang, L. J.; Qiu, S. R.; Zachowicz, W.; Guan, X. Y.; De Yoreo, J. J.; Nancollas, G. H.; Hoyer, J. R. *Langmuir* **2006**, *22*, 7279.

(66) Bramley, A. S.; Hounslow, M. J.; Ryall, R. L. *Chem. Eng. Sci.* **1997**, *52*, 747.

(67) Azzopardi, P. V.; O'Young, J.; Lajoie, G.; Karttunen, M.; Goldberg, H. A.; Hunter, G. K. *PLoS One* **2010**, *5*, e9330.